

# Chunking the Critic: A Transformer-based Soft Actor-Critic with N-Step Returns

Dong Tian, Ge Li, Hongyi Zhou, Onur Celik, Gerhard Neumann

**Keywords:** Transformer as Critic Network, N-steps return, Soft Actor-Critic, Critic Chunking

## Summary

This paper introduces a novel approach for improving Soft Actor-Critic (SAC) performance by integrating N-returns within a Transformer-based critic network. Unlike traditional methods that focus on evaluating single state-action pairs or apply action chunking in the actor network, this approach feeds chunked actions directly into the critic. Leveraging the Transformer's strength in processing sequential data, the proposed architecture achieves more robust value estimation. Empirical evaluations demonstrate that this method leads to efficient and stable training, particularly excelling in environments with sparse rewards or Multi-Phase tasks.

## Contribution(s)

1. We present a novel critic architecture for SAC that leverages Transformers to process sequential information, resulting in more accurate value estimations.  
**Context:** Transformer-Based Critic Network
2. We introduce a method for incorporating N-Step returns into the critic network in a stable and efficient manner, effectively mitigating the common challenges of variance and importance sampling associated with N-returns.  
**Context:** Stable Integration of N>Returns
3. We shift action chunking from the actor to the critic, demonstrating that enhanced temporal reasoning at the critic level—beyond traditional actor-side exploration—drives performance improvements in sparse and multi-phase tasks.  
**Context:** Unlike previous approaches that focus on actor-side chunking for exploration, our Transformer-based critic network produces a smooth value surface that is highly responsive to dataset variations, eliminating the need for additional exploration enhancements.
4. We empirically validate our approach, demonstrating significant improvements in training stability and overall performance, especially in challenging environments with sparse rewards and multi-phase tasks.  
**Context:** Our method achieves state-of-the-art performance on benchmarks such as Metaworld-ML1 and Box-Pushing Sparse, excelling in challenging tasks like Disassemble, Assembly, and Stick-Pull.

# Chunking the Critic: A Transformer-based Soft Actor-Critic with N-Step Returns

Dong Tian<sup>1</sup>, Ge Li<sup>1</sup>, Hongyi Zhou<sup>1</sup>, Onur Celik<sup>1</sup>, Gerhard Neumann<sup>1</sup>

Dong.Tian@student.kit.edu

<sup>1</sup>Karlsruhe Institute of Technology

## Abstract

Soft Actor-Critic (SAC) critically depends on its critic network, which typically evaluates a single state-action pair to guide policy updates. Using N-step returns is a common practice to reduce the bias in the target values of the critic. However, using N-step returns can again introduce high variance and necessitates importance sampling, often destabilizing training. Recent algorithms have also explored action chunking—such as direct action repetition and movement primitives—to enhance exploration. In this paper, we propose a **Transformer-based Critic Network** for SAC that integrates the N-returns framework in a stable and efficient manner. Unlike approaches that perform chunking in the actor network, we feed chunked actions into the critic network to explore potential performance gains. Our architecture leverages the Transformer’s ability to process sequential information, facilitating more robust value estimation. Empirical results show that this method not only achieves efficient, stable training but also excels in sparse reward/multi-phase environments—traditionally a challenge for step-based methods. These findings underscore the promise of combining Transformer-based critics with N-returns to advance reinforcement learning performance

## 1 Introduction

Reinforcement Learning (RL) has demonstrated remarkable success in a variety of domains, including robotic control, game playing, and complex decision-making tasks. Among the many RL algorithms, Soft Actor-Critic (SAC) (Haarnoja et al., 2018a) has emerged as a leading method for continuous control because of its sample efficiency and stable learning dynamics. Building on these advances, CrossQ (Bhatt et al., 2019) introduced Batch Renormalization (BRN) (Ioffe, 2017), an enhanced variant of Batch Normalization (Ioffe, 2015), together with bounded activation functions that eliminate the need for a target network, thereby achieving state-of-the-art performance and unprecedented sample efficiency.

Movement primitives, which typically generate chunked actions, have also enjoyed considerable success in RL (Otto et al., 2023; Li et al., 2024b). In contrast, step-based methods often produce jerky actions and suffer from a limited exploration space (Zhang et al., 2022). Although Sharma et al. (2017) proposed a method that enables an agent to determine both the action and the time scale of its repetition, and Zhang et al. (2022) employed a Gated Recurrent Unit (GRU) (Cho et al., 2014) as the actor network, these approaches have not yielded outstanding results.

A persistent challenge in RL is the accurate estimation of the  $Q$ -function, particularly in environments characterized by sparse rewards, long horizons, or high-dimensional state and action spaces. Multi-step return methods, such as *N-step returns* (Sutton, 2018), have been proposed to improve target value estimates by incorporating additional return information. However, these methods can increase variance and require importance sampling corrections to maintain unbiasedness, thereby adding complexity that may destabilize training.

Motivated by these challenges, we investigate whether action chunking can be effectively integrated within the critic network. Rather than processing individual state-action pairs  $(s_t, a_t)$ , our approach inputs sequences of actions  $(s_t, a_t, a_{t+1}, \dots, a_{t+N})$  directly into the critic. Instead of just predicting the Q-Value of the current action, the critic is now tasked to predict the K-step returns for all  $K = 1 \dots N$ . Traditional recurrent neural networks, such as GRUs, are limited by issues like gradient vanishing and the need for sequential processing, which hampers parallelization. In contrast, the Transformer-based Off-Policy Episodic Reinforcement Learning (TOP-ERL) framework (Li et al., 2024a) demonstrates that Transformers offer a promising alternative for constructing critic networks.

Inspired by these insights, we designed a Transformer-based Critic Network and integrated it into the Soft Actor-Critic framework. This **Transformer-based Soft Actor-Critic (T-SAC)** not only enhances performance but also contributes to more stable training dynamics.

## 2 Related Work and Background

### 2.1 Off-Policy Reinforcement Learning and SAC

Off-policy Reinforcement Learning (Sutton, 2018) improves sample efficiency through experience replay while decoupling behavior and target policies. Among modern off-policy algorithms, **Soft Actor-Critic (SAC)** (Haarnoja et al., 2018a) has become prominent for continuous control due to three key features:

- (i) Entropy-maximization for exploration via the objective  $\mathbb{E}[Q(s, a) - \alpha \log \pi(a|s)]$  (Ziebart et al., 2008)
- (ii) Twin Q-networks with target smoothing to combat overestimation bias (Hasselt, 2010)
- (iii) Automatic entropy coefficient tuning for dynamic exploration-exploitation balance (Haarnoja et al., 2018b)

This combination enables stable learning in high-dimensional spaces while maintaining sample efficiency - a critical advantage for real-world control applications.

### 2.2 Transformer-based Critics for Episodic RL

**Transformer-based Off-Policy Episodic RL (TOP-ERL)** (Li et al., 2024a) introduces architectural innovation through a transformer-based critic that processes trajectory segments rather than full episodes. Unlike conventional episodic RL approaches (Otto et al., 2023; Li et al., 2024b) that treat trajectories as monolithic sequences, TOP-ERL’s critic employs attention mechanisms to model  $N$ -step temporal dependencies, decomposes trajectories into overlapping segments for parallelized credit assignment, and uses positional encoding to preserve temporal ordering without recurrence. In this paper, we adopt a similar approach for learning the critic, leveraging trajectory data and learning from  $N$ -step returns without the need of importance sampling. Yet, we introduce a step-based policy instead of the episodic policy used in TOP-ERL, allowing us to again learn fully reactive feedback policies.

### 2.3 Variance-Reduced $N$ -Step Returns

The  $N$ -step return target (Sutton, 2018)

$$G^{(N)} = \sum_{k=0}^{N-1} \gamma^k r_k + \gamma^N V_\phi(s_{k+N}) \quad (1)$$

combines immediate rewards with bootstrapped value estimates. Ignoring discounting ( $\gamma = 1$ ), for (approximately) i.i.d. rewards  $r_k \sim (\mu, \Sigma)$ , the Central Limit Theorem (CLT) (Feller, 1991) gives

$$\sum_{k=0}^{N-1} r_k \sim \mathcal{N}(N\mu, N\Sigma), \quad (2)$$

leading to variance growth linear in  $N$  and damage the training result (Nauman et al., 2024).

**Averaged  $N$ -Step Targets** One solution is to compute expectations over partial returns, i.e.,

$$\bar{G}^{(N)} = \frac{1}{N} \sum_{i=1}^N G^{(i)}. \quad (3)$$

Assuming no discounting (i.e.,  $\gamma = 1$ ), we obtain

$$\text{Var}(\bar{G}^{(N)}) \approx \Sigma \left[ \frac{(N+1)(2N+1)}{6N} \right] + \frac{\Sigma_V}{N}, \quad (4)$$

where  $\Sigma_V$  denotes the value function’s estimation variance. The analysis shows that the variance of the reward summation term reduces from  $\mathcal{O}(N)$  to  $\mathcal{O}(N/3)$ , and the term  $\frac{\Sigma_V}{N}$ —which represents the estimation variance of the value function—vanishes as  $N$  increases. The complete derivation is provided in Appendix B.

**Practical Implementation for Sparse Rewards** Sparse reward environments—ubiquitous in many real-world applications—pose unique challenges for the averaging  $N$ -step return methods mentioned above. Two primary issues arise:

1. **Signal Dilution:** In scenarios where rewards are predominantly zero, direct averaging of  $N$ -step targets can yield uninformative estimates.
2. **Variable Target Consistency:** Allowing  $N$  to vary across episodes may lead to inconsistent target estimates, potentially destabilizing learning.

To address these challenges, our approach decouples the averaging process from the target value computation 3.1. Rather than directly averaging the  $N$ -step returns, we compute distinct target values for different  $N$  and aggregate the resulting gradients during backpropagation. Although the targets themselves may differ, the shared neural network processes these gradients in an averaged manner, thus preserving the variance reduction benefits without suffering from the drawbacks of diluted signals.

As demonstrated in Section 4, our gradient-level averaging strategy not only preserves the variance-reduction benefits but also substantially improves both stability and success rates, particularly in environments with sparse rewards. For a comprehensive explanation of this approach, please refer to Paragraph 3.1.

### 3 The Transformer-based Soft Actor-Critic

Figure 1 illustrates our Policy and Critic networks. Unlike conventional SAC, which stores individual state–action pairs (Haarnoja et al., 2018a), our approach archives entire trajectories as single data points and compute  $N$ -step returns for these trajectories. The transformer critic then has to predict the  $N$ -step returns given the next  $N$  actions in the trajectory. Algorithm 1 summarizes the T-SAC pipeline. The agent collects full trajectories during interaction with the environment, which are stored in a replay buffer. During training, batches of trajectories are sampled to compute  $N$ -step return targets which are used to update the Transformer-based Critic. Subsequently, policy parameters are adjusted and the alpha parameter is automatically tuned. Finally, the target network is updated via a soft update scheme.

#### 3.1 $N$ -Step Returns for Critic Updates

Our Critic (see Figure 1) produces  $Q$ -value estimates for every partial action sequence in a trajectory, following Zhang et al. (2022):

$$Q_\phi(s_t^k, a_t^k), Q_\phi(s_t^k, a_t^k, a_{t+1}^k), \dots, Q_\phi(s_t^k, a_t^k, \dots, a_{t+n-1}^k),$$

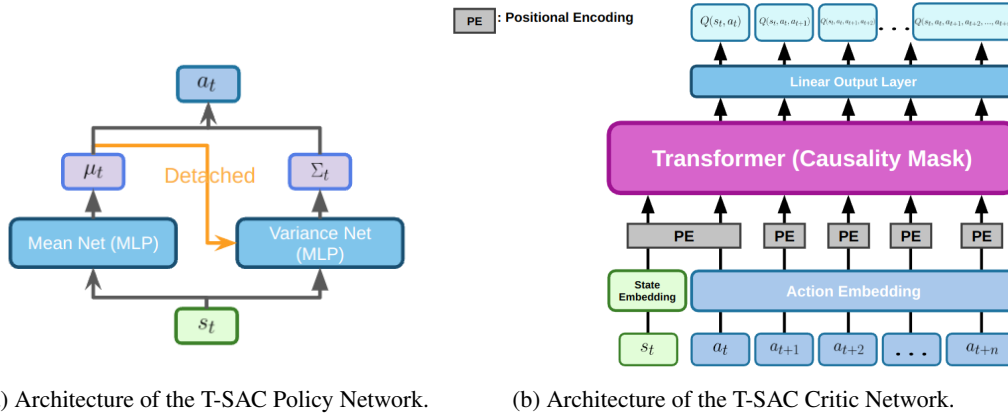
where  $\phi$  denotes the critic parameters. Each trajectory in a mini-batch of size  $L$  consists of  $N$  time steps:

$$\{(s_0^k, \dots, s_N^k, a_0^k, \dots, a_{N-1}^k, r_0^k, \dots, r_{N-1}^k)\}_{k=1}^L.$$

**N-Step Returns** For each update step, we randomly select an episode within a trajectory, starting at time step  $t$  (with  $t \in [0, N - n]$ ). The  $n$ -step return is defined as:

$$G^{(n)}(s_t^k, a_t^k, \dots, a_{t+n-1}^k) = \sum_{j=0}^{n-1} \gamma^j r_{t+j}^k + \gamma^n V_{\phi_{\text{tar}}}(s_{t+n}^k), \quad (5)$$

where  $r_{t+j}^k$  is the reward at step  $t + j$  in trajectory  $k$ ,  $\gamma$  is the discount factor,  $V_{\phi_{\text{tar}}}$  is the value function computed by a fixed target network, and  $s_{t+n}^k$  is the state reached after executing  $n$  actions from step  $t$  in trajectory  $k$ .



(a) Architecture of the T-SAC Policy Network.

(b) Architecture of the T-SAC Critic Network.

Figure 1: Overview of the T-SAC Network Architecture: Policy and Critic Networks.

---

### Algorithm 1: T-SAC Algorithm

---

**Initialize:** Critic parameters  $\phi$ , target critic  $\phi_{\text{target}} \leftarrow \phi$ , policy parameters  $\theta$ , and replay buffer  $\mathcal{B}$ . Reset environment to obtain  $s_0$ .

**repeat**

    // Collect trajectories

**repeat**

        Sample action  $a_t \sim \pi_\theta(\cdot | s_t)$  and observe  $(r_t, s_{t+1}, d_t)$ .

        Store  $(s_t, a_t, r_t, s_{t+1}, d_t)$  in a temporary buffer.

$s_t \leftarrow s_{t+1}$ .

**until** until episode termination;

    Store the full trajectory in  $\mathcal{B}$ .

    // Perform updates

**for** each update step **do**

        // Critic update:

        Sample a batch of trajectories from  $\mathcal{B}$ , compute the N-step return targets, and update the Transformer Critic.

        // Policy update:

        Update  $\theta$  and the temperature parameter using the same batch.

        // Target network update:

$\phi_{\text{target}} \leftarrow \tau\phi + (1 - \tau)\phi_{\text{target}}$ .

**end**

**until** until convergence;

---

**Critic Training Objective** Given the next  $n$  actions, our critic is tasked to output the  $N$ -step returns. Note that we use a causal transformer architecture where we can feed the next  $n$  actions as tokens and the critic needs all  $N$ -step returns (from 1 to  $n$ ) for this action sequence. The critic is trained by minimizing the mean squared error (MSE) between its Q-value estimates and the corresponding  $N$ -step returns:

$$\mathcal{L}(\phi) = \frac{1}{L \cdot n} \sum_{k=1}^L \sum_{i=0}^{n-1} \left[ Q_{\phi}(s_t^k, a_t^k, \dots, a_{t+i}^k) - G^{(n)}(s_t^k, a_t^k, \dots, a_{t+i}^k) \right]^2, \quad (6)$$

where  $t$  is randomly selected for each update ( $t \in [0, N - n]$ ) and  $n$  ranges from  $min\_length$  to  $max\_length$ .

**How the Benefit of Averaging is Leveraged** Although the critic loss in Eq. (6) uses  $N$ -step returns, our method *does not* directly average these returns. Instead, for each training sample, we compute distinct  $n$ -step targets  $G^{(1)}, G^{(2)}, \dots, G^{(n)}$  and form separate loss terms

$$\mathcal{L}_1(\phi), \quad \mathcal{L}_2(\phi), \quad \dots, \quad \mathcal{L}_n(\phi),$$

These losses are then *aggregated at the gradient level* rather than at the target level. Concretely, if  $\nabla_{\phi} \mathcal{L}_i(\phi)$  denotes the gradient of the loss term corresponding to the  $i$ -th  $N$ -step target  $G^{(i)}$ , we update the parameters  $\phi$  via

$$\nabla_{\phi} \bar{\mathcal{L}}(\phi) = \frac{1}{n} \sum_{i=1}^n \nabla_{\phi} \mathcal{L}_i(\phi). \quad (7)$$

By averaging *gradients* instead of *returns*, the critic still benefits from the variance-reduction properties of using multiple  $N$ -step returns while avoiding the dilution of any sparse reward signals.

This perspective also explains why the outputs of our Transformer Critic are

$$Q_{\phi}(s_t^k, a_t^k), \quad Q_{\phi}(s_t^k, a_t^k, a_{t+1}^k), \quad \dots, \quad Q_{\phi}(s_t^k, a_t^k, \dots, a_{t+n-1}^k),$$

rather than

$$Q_{\phi}(s_t^k, a_t^k), \quad Q_{\phi}(s_{t+1}^k, a_{t+1}^k), \quad \dots, \quad Q_{\phi}(s_{t+n}^k, a_{t+n-1}^k).$$

Were we to shift the Q-value inputs forward in time instead, we could not apply gradient-level averaging in the same manner; hence, we would lose the benefits of variance reduction gained from combining multiple  $N$ -step targets.

### 3.2 Policy Network and Objective

Our policy network largely follows the original SAC design, with two key modifications for improved performance and stability:

**Design Choice 1: Incorporating the Mean Action into the Covariance Network.** The policy’s mean action  $\mu_t$  is fed as a detached input into the covariance network. This allows the network to recognize shifts toward novel actions—even in familiar states—thereby maintaining or increasing the estimated variance. This approach prevents the network from collapsing to narrow distributions and promotes robust exploration.

**Design Choice 2: Layer Normalization.** Layer normalization is applied to both the mean and variance sub-networks. For the mean network, normalization avoids excessively large or small outputs, thereby preventing gradient issues. For the variance network, it mitigates variance shrinkage when encountering similar states and actions repeatedly, ensuring sustained exploratory noise.

**Policy Update Objective** Following the standard SAC approach (Haarnoja et al., 2018a), the policy parameters  $\theta$  are updated by minimizing:

$$J_{\pi}(\theta) = \mathbb{E}_{s_t \sim \mathcal{D}, a_t \sim \pi_{\theta}} \left[ \alpha \log \pi_{\theta}(a_t | s_t) - Q_{\phi}(s_t, a_t) \right]. \quad (8)$$

The temperature parameter  $\alpha$  is adjusted to achieve a target entropy  $-\bar{\mathcal{H}}$  (typically set to  $-\dim(\mathcal{A})$  as in standard SAC) (Haarnoja et al., 2018b), where  $\mathcal{A}$  represents action space:

$$J(\alpha) = \mathbb{E}_{s_t \sim \mathcal{D}, a_t \sim \pi_{\theta}} \left[ -\alpha (\log \pi_{\theta}(a_t | s_t) + \bar{\mathcal{H}}) \right]. \quad (9)$$

These architectural innovations—trajectory-level data storage, a Transformer-based critic, and a refined policy network—collectively enhance sample efficiency and robustness in continuous control tasks.

## 4 Experiments results and ablation study

We evaluated our T-SAC algorithm on two challenging benchmarks. The first benchmark is Metaworld-ML1 (Yu et al., 2020), a suite of tasks designed to test both learning efficiency and generalization. The second benchmark consists of dense and sparse Box-Pushing tasks from `fancy_gym` (Otto et al.), which impose tight positional ( $\pm 5$  mm) and angular ( $\pm 0.5$  rad) constraints. Table 1 and Figure 4.2 illustrate T-SAC’s performance on these tasks, highlighting its robustness and generalization capabilities.

### 4.1 Metaworld Results

In Metaworld-ML1, T-SAC consistently outperforms competing algorithms, particularly on multi-phase tasks such as *Assembly*, *Disassemble*, and *Hammer*, which require sequential manipulation skills. Methods such as PPO or SAC may learn certain tasks well but often fail to generalize to a broad range of tasks. In contrast, T-SAC maintains strong performance across all tasks, achieving an overall success rate that is 16% higher than the second-best method (SAC). Detailed, per-task performance metrics can be found in Appendix A.

### 4.2 Box Pushing (Dense and Sparse)

Box-pushing tasks have traditionally been explored using control methodologies such as Model Predictive Control (MPC) (Arruda et al., 2017), which excel at enforcing constraints when system dynamics are well-characterized. However, MPC entails repeatedly solving an optimization problem at each timestep, incurring high computational overhead, and can struggle with timing and robustness, particularly when joint-space dynamics must be inferred for precise task-space control.

Reinforcement learning (RL) approaches tend to learn these tasks faster, although prior algorithms have struggled to exceed 85% success due to the dual-objective constraints of meeting specific positional and angular tolerances. T-SAC surpasses this threshold, achieving a 92% success rate under dense rewards and 58% under sparse rewards. These results set a new performance benchmark for box-pushing tasks and confirm T-SAC’s capacity to handle complex dual-objective requirements in real-world-inspired robotic control scenarios.

### 4.3 Ablation Study

To elucidate the contributions of each component, we conducted ablation experiments on a carefully selected subset of Metaworld tasks that span a diverse range of manipulation challenges. The results are presented in Figure 3..

Table 1: Test Results: Average Success Rate (%) for Different Algorithms on Metaworld-ML1 and Box Pushing Benchmarks

	PPO	gSDE	GTrXL	SAC	CrossQ	T-SAC
Metaworld Overall Success Rate (%)	70	68	63	70	50	<b>86</b>
Box Pushing Dense (%)	2	60	52	18	0	<b>92</b>
Box Pushing Sparse (%)	3	<b>60</b>	0	0	0	58

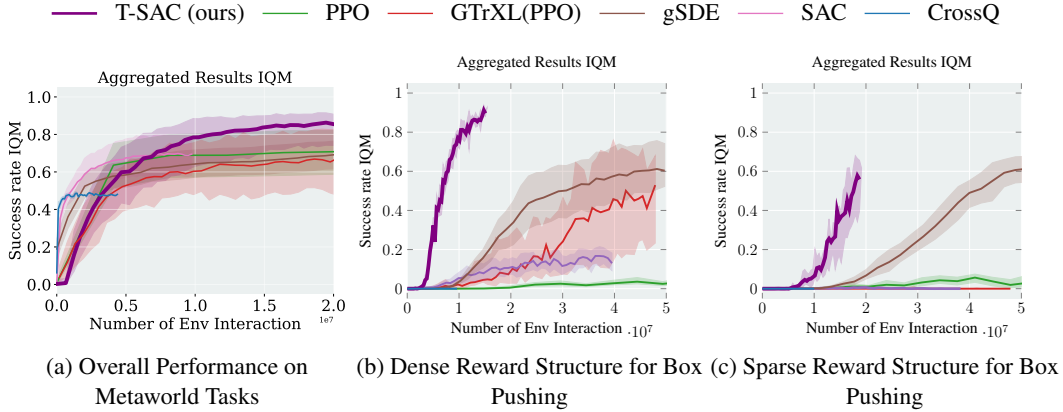


Figure 2: Comparative evaluation of performance metrics across two benchmarks. Panel (a) shows the aggregate results for Metaworld tasks, whereas panels (b) and (c) present the success rate of the Box Pushing task under dense and sparse reward regimes, respectively.

### 4.3.1 Feeding the Mean to the Covariance Network

This experiment was conducted on 11 tasks (Basketball, Box-Close, Button-Press, Button-Press-Wall, Coffee-Push, Disassemble, Faucet-Open, Hand-insert, Plate-Slide-Back, Push, Reach). Incorporating the mean into the covariance network did not substantially affect performance when measured with the IQM metric (requiring 75% convergence). However, it reduced the variance across different random seeds, leading to more consistent outcomes.

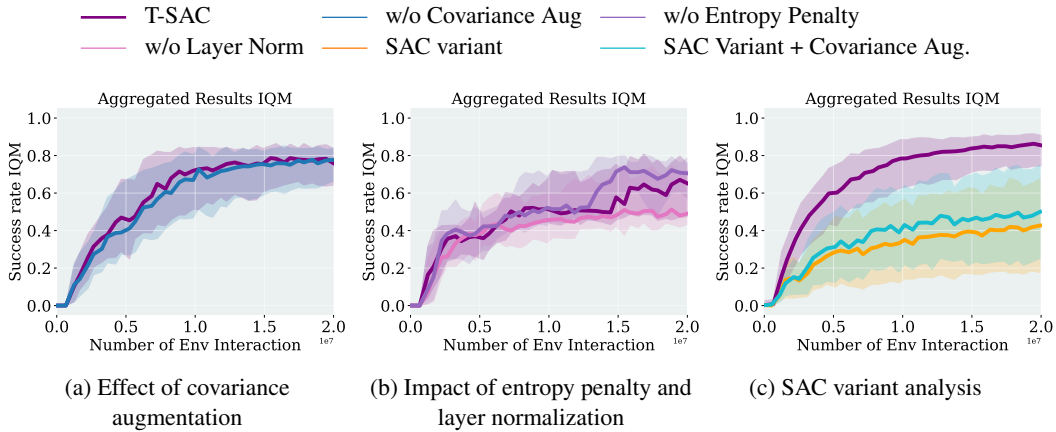


Figure 3: Ablation studies comparing different model configurations.

### 4.3.2 Layer Normalization in the Policy Network

The experiment was conducted on 5 tasks (Assembly, Button-Press, Coffee-Push, Faucet-open, Reach). Applying layer normalization within the policy network improved success rates. The stabilization provided by normalization appears to enhance training robustness.

### 4.3.3 Entropy Term: Inclusion vs. Removal

This test was conducted on 5 tasks (Assembly, Button-Press, Coffee-Push, Faucet-open, Reach). The SAC algorithm traditionally employs an entropy term to promote exploration. We investigated the impact of removing this term, effectively transitioning toward a hard Actor-Critic framework. On the *assembly-v2* task, removing the entropy term (yielding a Transformer-based Hard Actor-Critic) resulted in convergence in 7 out of 8 runs, whereas the standard Transformer-based SAC configuration (retaining the entropy term) converged in 5 out of 8 runs. Although the entropy term fosters exploration, it may also introduce off-target samples into the replay buffer, potentially slowing convergence due to the Transformer-based critic’s sensitivity to distributional shifts. While removing the entropy term can yield improved performance on select tasks, caution is warranted due to the risk of overfitting to limited behavioral modes. Future work should explore adaptive strategies, such as selectively disabling the entropy term during later training stages to better balance exploration and exploitation.

### 4.3.4 SAC Variant

To isolate our contribution, we propose a SAC variant that integrates our T-SAC framework while substituting the Transformer-based Critic with the original MLP-based Critic. We also examine an alternative version that incorporates our augmented covariance network. Both variants use the same configuration as T-SAC, featuring an Update-to-Data (UTD) ratio of 0.25 and a training schedule that begins with 100 critic updates followed by 20 policy updates. The aggregated success rates across all 50 Metaworld tasks, presented in the Figure 3, highlight the performance improvements achieved through these design choices.

## 5 Conclusion and Future Work

Our T-SAC framework establishes a new state-of-the-art for multiphase and box-pushing tasks by significantly outperforming traditional step-based approaches. By integrating a transformer-based critic, our framework approximates a smooth, globally coherent objective function that captures temporal dependencies and produces continuous control sequences. In contrast, multiphase methods typically rely on open-loop control, while step-based methods often neglect historical control signals. To the best of our knowledge, no existing method successfully combines the advantages of both approaches without inheriting their drawbacks. Additionally, with advancements in search-based techniques, the efficiency of gradient descent optimization may be diminishing.

Motivated by these insights, our future work will focus on two main objectives. First, we plan to develop policies that generate action sequences informed by past states. By incorporating recurrent or transformer-based memory alongside temporal abstraction, we aim to enhance robustness in perturbed environments. Second, we intend to explore advanced optimization techniques such as natural gradients and trust region-based methods to improve convergence rates and more effectively traverse the critic’s return landscape while maintaining computational efficiency. These efforts are designed to leverage the strengths of both multiphase and step-based methods while mitigating their individual limitations.

## A Appendix : Individual Metaworld results

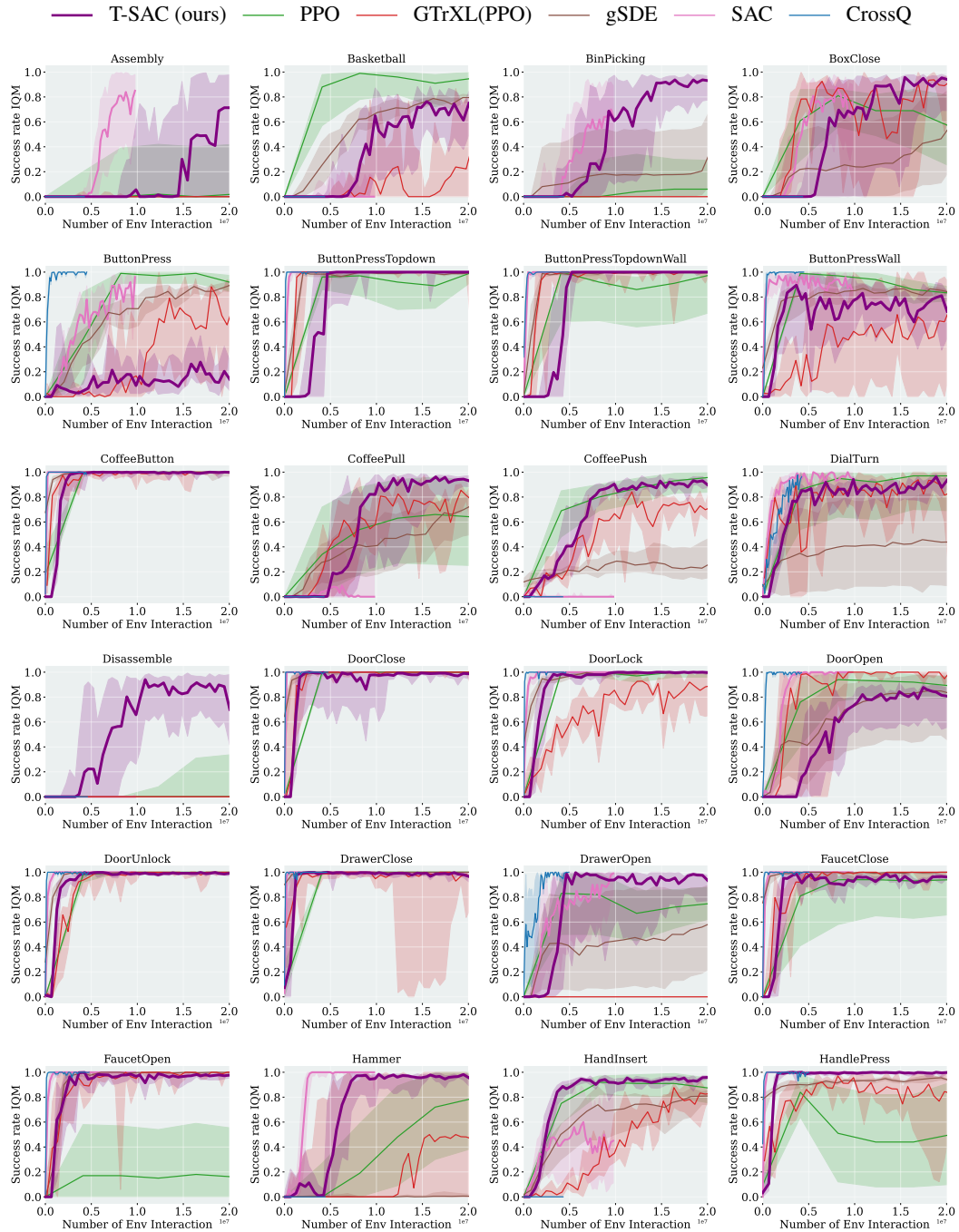


Figure 4: Success Rate IQM of each individual Metaworld tasks. (Part 1)

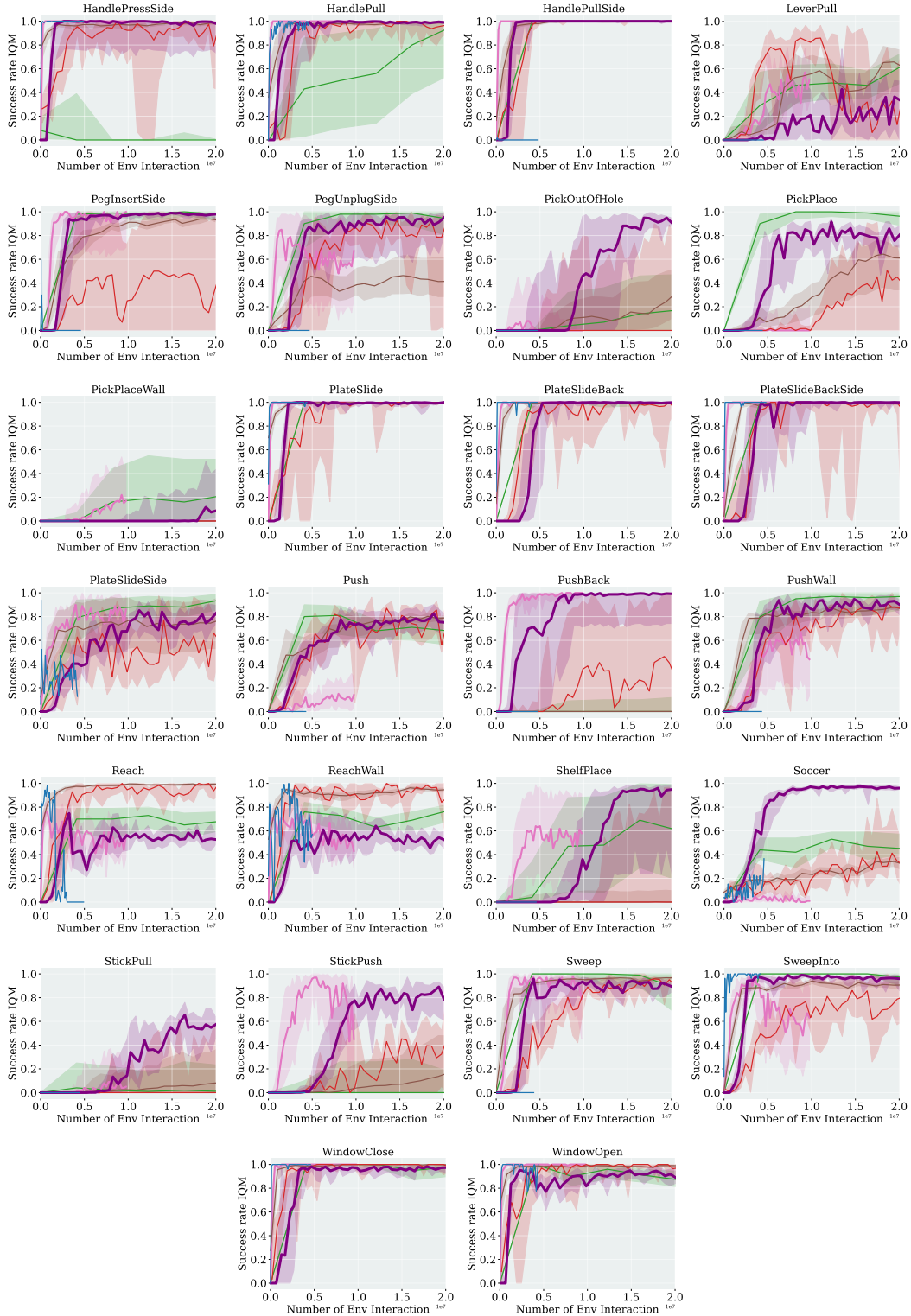


Figure 5: Success Rate IQM of each individual Metaworld tasks. (Part 2)

## B Appendix: Average of N-steps return

Notice that in

$$\frac{1}{N} \sum_{i=0}^N \sum_{k=0}^{i-1} r_k,$$

each reward  $r_k$  (for  $k = 0, \dots, N-1$ ) appears in exactly  $(N-k)$  of the inner sums. We can rewrite the double sum in “triangular” form:

$$\frac{1}{N} \sum_{i=0}^N \sum_{k=0}^{i-1} r_k = \frac{1}{N} \sum_{k=0}^{N-1} (N-k) r_k.$$

Suppose the rewards  $r_k$  are (approximately) i.i.d. with mean  $\mu$  and variance  $\sigma^2$ . Then:

$$\begin{aligned} \mathbb{E}\left[\frac{1}{N} \sum_{k=0}^{N-1} (N-k) r_k\right] &= \frac{1}{N} \sum_{k=0}^{N-1} (N-k) \mathbb{E}[r_k] \\ &= \frac{1}{N} \sum_{k=0}^{N-1} (N-k) \mu \\ &= \frac{\mu}{N} \sum_{j=1}^N j = \frac{\mu}{N} \cdot \frac{N(N+1)}{2} = \frac{N+1}{2} \mu. \end{aligned}$$

$$\begin{aligned} \text{Var}\left(\frac{1}{N} \sum_{k=0}^{N-1} (N-k) r_k\right) &= \frac{1}{N^2} \sum_{k=0}^{N-1} (N-k)^2 \text{Var}(r_k) \\ &= \frac{\sigma^2}{N^2} \sum_{k=0}^{N-1} (N-k)^2 \\ &= \frac{\sigma^2}{N^2} \sum_{j=1}^N j^2 = \frac{\sigma^2}{N^2} \cdot \frac{N(N+1)(2N+1)}{6} \\ &= \sigma^2 \frac{(N+1)(2N+1)}{6N}. \end{aligned}$$

For the approximate distribution via the Central Limit Theorem (CLT):

$$\begin{aligned} \sum_{k=0}^{N-1} (N-k) r_k &\sim \mathcal{N}\left(\mu \cdot \frac{N(N+1)}{2}, \sigma^2 \cdot \frac{N^2(N+1)(2N+1)}{6}\right), \\ \frac{1}{N} \sum_{k=0}^{N-1} (N-k) r_k &\sim \mathcal{N}\left(\frac{N+1}{2} \mu, \sigma^2 \frac{(N+1)(2N+1)}{6N}\right). \end{aligned}$$

## References

- Ermanno Arruda, Michael J Mathew, Marek Kopicki, Michael Mistry, Morteza Azad, and Jeremy L Wyatt. Uncertainty averse pushing with model predictive path integral control. In *2017 IEEE-RAS 17th International Conference on Humanoid Robotics (Humanoids)*, pp. 497–502. IEEE, 2017.
- Aditya Bhatt, Daniel Palenicek, Boris Belousov, Max Argus, Artemij Amiranashvili, Thomas Brox, and Jan Peters. Crossq: Batch normalization in deep reinforcement learning for greater sample efficiency and simplicity. *arXiv preprint arXiv:1902.05605*, 2019.
- Kyunghyun Cho, Bart Van Merriënboer, Caglar Gulcehre, Dzmitry Bahdanau, Fethi Bougares, Holger Schwenk, and Yoshua Bengio. Learning phrase representations using rnn encoder-decoder for statistical machine translation. *arXiv preprint arXiv:1406.1078*, 2014.
- William Feller. *An introduction to probability theory and its applications, Volume 2*, volume 2. John Wiley & Sons, 1991.
- Tuomas Haarnoja, Aurick Zhou, Pieter Abbeel, and Sergey Levine. Soft actor-critic: Off-policy maximum entropy deep reinforcement learning with a stochastic actor. In *International conference on machine learning*, pp. 1861–1870. PMLR, 2018a.
- Tuomas Haarnoja, Aurick Zhou, Kristian Hartikainen, George Tucker, Sehoon Ha, Jie Tan, Vikash Kumar, Henry Zhu, Abhishek Gupta, Pieter Abbeel, et al. Soft actor-critic algorithms and applications. *arXiv preprint arXiv:1812.05905*, 2018b.
- Hado Hasselt. Double q-learning. *Advances in neural information processing systems*, 23, 2010.
- Shengyi Huang, Rousslan Fernand Julien Dossa, Antonin Raffin, Anssi Kanervisto, and Weixun Wang. The 37 implementation details of proximal policy optimization. *The ICLR Blog Track 2023*, 2022.
- Sergey Ioffe. Batch normalization: Accelerating deep network training by reducing internal covariate shift. *arXiv preprint arXiv:1502.03167*, 2015.
- Sergey Ioffe. Batch renormalization: Towards reducing minibatch dependence in batch-normalized models. *Advances in neural information processing systems*, 30, 2017.
- Ge Li, Dong Tian, Hongyi Zhou, Xinkai Jiang, Rudolf Lioutikov, and Gerhard Neumann. Top-erl: Transformer-based off-policy episodic reinforcement learning. *arXiv preprint arXiv:2410.09536*, 2024a.
- Ge Li, Hongyi Zhou, Dominik Roth, Serge Thilges, Fabian Otto, Rudolf Lioutikov, and Gerhard Neumann. Open the black box: Step-based policy updates for temporally-correlated episodic reinforcement learning. *arXiv preprint arXiv:2401.11437*, 2024b.
- Michal Nauman, Mateusz Ostaszewski, Krzysztof Jankowski, Piotr Miłoś, and Marek Cygan. Bigger, regularized, optimistic: scaling for compute and sample-efficient continuous control. *arXiv preprint arXiv:2405.16158*, 2024.
- Fabian Otto, Onur Celik, Dominik Roth, and Hongyi Zhou. Fancy gym. URL [https://github.com/ALRhub/fancy\\_gym](https://github.com/ALRhub/fancy_gym).
- Fabian Otto, Onur Celik, Hongyi Zhou, Hanna Ziesche, Vien Anh Ngo, and Gerhard Neumann. Deep black-box reinforcement learning with movement primitives. In *Conference on Robot Learning*, pp. 1244–1265. PMLR, 2023.
- Emilio Parisotto, Francis Song, Jack Rae, Razvan Pascanu, Caglar Gulcehre, Siddhant Jayakumar, Max Jaderberg, Raphael Lopez Kaufman, Aidan Clark, Seb Noury, et al. Stabilizing transformers for reinforcement learning. In *International conference on machine learning*, pp. 7487–7498. PMLR, 2020.

- 
- Antonin Raffin and Freek Stulp. Generalized state-dependent exploration for deep reinforcement learning in robotics. *Arxiv*, 2020.
- Antonin Raffin, Ashley Hill, Adam Gleave, Anssi Kanervisto, Maximilian Ernestus, and Noah Dornmann. Stable-baselines3: Reliable reinforcement learning implementations. *Journal of machine learning research*, 22(268):1–8, 2021.
- John Schulman, Filip Wolski, Prafulla Dhariwal, Alec Radford, and Oleg Klimov. Proximal policy optimization algorithms. *arXiv preprint arXiv:1707.06347*, 2017.
- Sahil Sharma, Aravind Srinivas, and Balaraman Ravindran. Learning to repeat: Fine grained action repetition for deep reinforcement learning. *arXiv preprint arXiv:1702.06054*, 2017.
- Richard S Sutton. Reinforcement learning: An introduction. *A Bradford Book*, 2018.
- Tianhe Yu, Deirdre Quillen, Zhanpeng He, Ryan Julian, Karol Hausman, Chelsea Finn, and Sergey Levine. Meta-world: A benchmark and evaluation for multi-task and meta reinforcement learning. In *Conference on robot learning*, pp. 1094–1100. PMLR, 2020.
- Haichao Zhang, Wei Xu, and Haonan Yu. Generative planning for temporally coordinated exploration in reinforcement learning. *arXiv preprint arXiv:2201.09765*, 2022.
- Brian D Ziebart, Andrew L Maas, J Andrew Bagnell, Anind K Dey, et al. Maximum entropy inverse reinforcement learning. In *Aaai*, volume 8, pp. 1433–1438. Chicago, IL, USA, 2008.

# Supplementary Materials

*The following content was not necessarily subject to peer review.*

## C Experiment Description

### C.1 Meta-World ML1

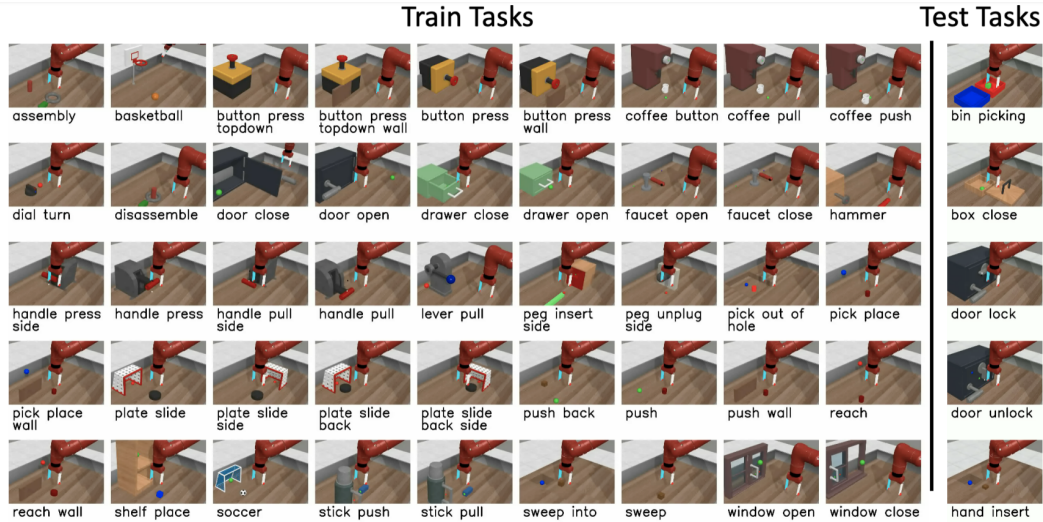


Figure 6: Metaworld Task (Yu et al. (2020))

MetaWorld (Yu et al., 2020) is an open-source simulated benchmark designed for both meta-reinforcement learning and multi-task learning in robotic manipulation. It consists of 50 unique manipulation tasks, each introducing distinct challenges that require robots to acquire a wide range of skills, such as grasping, pushing, and object placement. Unlike benchmarks that target a narrow range of tasks, MetaWorld offers a diverse array of challenges, making it an ideal platform for developing algorithms capable of generalizing across various behaviors. Figure 7 details each individual MetaWorld task, showcasing their varied types and complexities.

### C.2 Box Pushing

The Robot Box Pushing environment features a 7-DoF Franka Emika Panda arm, equipped with a rod, pushing a box to a designated target position and orientation. Both the robot’s joint states and the box’s pose are part of the observations, while torque commands at each joint form the actions. In the dense reward setting, feedback is continuously provided through multiple sub-rewards (e.g., box alignment, rod position, and action cost), guiding the learning process at every timestep. Conversely, the sparse reward setting only delivers the main task-related rewards (position and orientation errors) at the final timestep, making the task more challenging due to less frequent feedback.

## D Experimental Methodology

### D.1 Algorithm Implementations

In our study, we implement and compare several state-of-the-art reinforcement learning algorithms, each leveraging distinct mechanisms for policy optimization and exploration:

**Proximal Policy Optimization (PPO-Clip)** We adopt the PPO-Clip variant Schulman et al. (2017), using the implementation provided by Raffin et al. (2021). This approach utilizes a clipped surro-

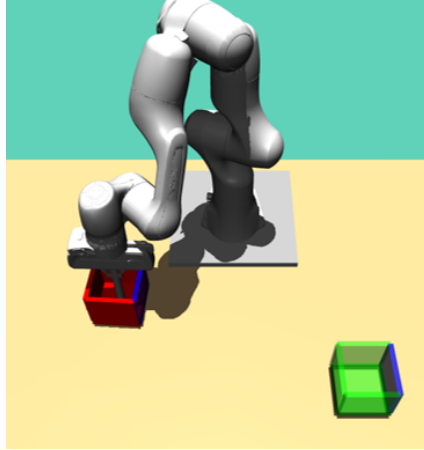


Figure 7: Box Pushing Task (Otto et al.)

gate objective to ensure stable policy updates while preventing large, destabilizing changes during optimization.

**Soft Actor-Critic (SAC)** Our off-policy baseline is based on the entropy-regularized SAC algorithm Haarnoja et al. (2018a), as implemented in Raffin et al. (2021). This method employs twin Q-networks and experience replay, thereby effectively balancing exploration and exploitation through entropy maximization.

**Gated Transformer-XL (GTrXL)** We implement the GTrXL architecture following the stabilizing techniques introduced by Parisotto et al. (2020) and further refined by Huang et al. (2022). Our version incorporates minibatch advantage normalization and a state-independent variance estimation to enhance learning stability and performance.

**Generalized State-Dependent Exploration (gSDE)** In line with the method described in Raffin & Stulp (2020), we generate temporally correlated noise via linear combinations of basis vectors sampled from a multivariate normal distribution,  $\theta_\epsilon \sim \mathcal{N}^d(0, \Sigma)$ . Additionally, we employ scheduled clip ranges to maintain stability throughout the learning process.

**CrossQ** Our implementation of CrossQ is adapted from the original code base presented in Bhatt et al. (2019).

## D.2 Hyperparameters of the algorithms

Table 2: Hyperparameters for the Meta-World experiments. Episode Length  $T = 500$

	PPO	gSDE	GTrXL	SAC	CrossQ	T-SAC
number samples	16000	16000	19000	1000	1	2000
GAE $\lambda$	0.95	0.95	0.95	n.a.	n.a.	n.a.
discount factor	0.99	0.99	0.99	0.99	0.99	0.99
optimizer	adam	adam	adam	adam	adam	adamw
epochs	10	10	5	1000	1	5
learning rate	3e-4	1e-3	2e-4	3e-4	3e-4	2.5e-4
use critic	True	True	True	True	True	True
epochs critic	10	10	5	1000	1	100
learning rate critic	3e-4	1e-3	2e-4	3e-4	3e-4	2.5e-5
number minibatches	32	n.a.	n.a.	n.a.	n.a.	n.a.
batch size	n.a.	500	1024	256	256	512
buffer size	n.a.	n.a.	n.a.	1e6	1e6	5000
learning starts	0	0	n.a.	10000	0	200
polyak_weight	n.a.	n.a.	n.a.	5e-3	n.a.	5e-3
SDE sampling frequency	n.a.	4	n.a.	n.a.	n.a.	n.a.
entropy coefficient	0	0	0	auto	auto	auto
normalized observations	True	True	False	False	False	False
normalized rewards	True	True	0.05	False	False	False
observation clip	10.0	n.a.	n.a.	n.a.	n.a.	n.a.
reward clip	10.0	10.0	10.0	n.a.	n.a.	n.a.
critic clip	0.2	lin_0.3	10.0	n.a.	n.a.	n.a.
importance ratio clip	0.2	lin_0.3	0.1	n.a.	n.a.	n.a.
min_length	n.a.	n.a.	n.a.	n.a.	n.a.	1
max_length	n.a.	n.a.	n.a.	n.a.	n.a.	16
hidden layers	[128, 128]	[128, 128]	n.a.	[256, 256]	[256, 256]	[128, 128]
hidden layers critic	[128, 128]	[128, 128]	n.a.	[256, 256]	[2048, 2048]	n.a.
hidden activation	tanh	tanh	relu	relu	relu	leaky_relu
orthogonal initialization	Yes	No	xavier	fanin	fanin	fanin
initial std	1.0	0.5	1.0	1.0	1.0	0.01
number of heads	-	-	4	-	-	4
dims per head	-	-	16	-	-	32
number of attention layers	-	-	4	-	-	2
max sequence length	-	-	5	-	-	1024

Table 3: Hyperparameters for the Box Pushing Dense, Episode Length  $T = 100$ 

	PPO	gSDE	GTrXL	SAC	crossq	T-SAC
number samples	48000	80000	8000	8	1	400
GAE $\lambda$	0.95	0.95	0.95	n.a.	n.a.	n.a.
discount factor	1.0	1.0	0.99	0.99	0.99	0.98
optimizer	adam	adam	adam	adam	adam	adamw
epochs	10	10	5	1	1	1
learning rate	5e-5	1e-4	2e-4	3e-4	3e-4	2.5e-4
use critic	True	True	True	True	True	True
epochs critic	10	10	5	1	1	100
learning rate critic	1e-4	1e-4	2e-4	3e-4	3e-4	3e-5
number minibatches	40	n.a.	n.a.	n.a.	n.a.	n.a.
batch size	n.a.	2000	1000	512	256	256
buffer size	n.a.	n.a.	n.a.	2e6	1e6	20000
learning starts	0	0	0	1e5	0	5000
polyak_weight	n.a.	n.a.	n.a.	5e-3	n.a.	0.002
SDE sampling frequency	n.a.	4	n.a.	n.a.	n.a.	n.a.
entropy coefficient	0	0.01	0	auto	auto	0
normalized observations	True	True	False	False	False	False
normalized rewards	True	True	0.1	False	False	False
observation clip	10.0	n.a.	n.a.	n.a.	n.a.	n.a.
reward clip	10.0	10.0	10.	n.a.	n.a.	n.a.
critic clip	0.2	0.2	10.	n.a.	n.a.	n.a.
importance ratio clip	0.2	0.2	0.1	n.a.	n.a.	n.a.
min_length	n.a.	n.a.	n.a.	n.a.	n.a.	1
max_length	n.a.	n.a.	n.a.	n.a.	n.a.	4
hidden layers	[512, 512]	[256, 256]	n.a.	[256, 256]	[256, 256]	[512 * 4]
hidden layers critic	[512, 512]	[256, 256]	n.a.	[256, 256]	[2048, 2048]	n.a.
hidden activation	tanh	tanh	relu	tanh	relu	leaky_relu
orthogonal initialization	Yes	No	xavier	fanin	fanin	Yes
initial std	1.0	0.05	1.0	1.0	1.0	1.0
number of heads	-	-	4	-	-	4
dims per head	-	-	16	-	-	64
number of attention layers	-	-	4	-	-	2
max sequence length	-	-	5	-	-	1024

Table 4: Hyperparameters for the Box Pushing Sparse, Episode Length  $T = 100$ 

	PPO	gSDE	GTrXL	SAC	crossq	T-SAC
number samples	48000	80000	8000	8	1	400
GAE $\lambda$	0.95	0.95	0.95	n.a.	n.a.	n.a.
discount factor	1.0	1.0	0.99	0.99	0.99	1.0
optimizer	adam	adam	adam	adam	adam	adamw
epochs	10	10	5	1	1	1
learning rate	5e-5	1e-4	2e-4	3e-4	3e-4	2.5e-4
use critic	True	True	True	True	True	True
epochs critic	10	10	5	1	1	100
learning rate critic	1e-4	1e-4	2e-4	3e-4	3e-4	3e-5
number minibatches	40	n.a.	n.a.	n.a.	n.a.	n.a.
batch size	n.a.	2000	1000	512	256	256
buffer size	n.a.	n.a.	n.a.	2e6	1e6	20000
learning starts	0	0	0	1e5	0	5000
polyak_weight	n.a.	n.a.	n.a.	5e-3	n.a.	2e-3
SDE sampling frequency	n.a.	4	n.a.	n.a.	n.a.	n.a.
entropy coefficient	0	0.01	0	auto	auto	0
normalized observations	True	True	False	False	False	False
normalized rewards	True	True	0.1	False	False	False
observation clip	10.0	n.a.	n.a.	n.a.	n.a.	n.a.
reward clip	10.0	10.0	10.	n.a.	n.a.	n.a.
critic clip	0.2	0.2	10.	n.a.	n.a.	n.a.
importance ratio clip	0.2	0.2	0.1	n.a.	n.a.	n.a.
hidden layers	[512, 512]	[256, 256]	n.a.	[256, 256]	[256, 256]	[512 * 4]
hidden layers critic	[512, 512]	[256, 256]	n.a.	[256, 256]	[2048, 2048]	n.a.
hidden activation	tanh	tanh	relu	tanh	relu	leaky_relu
orthogonal initialization	Yes	No	xavier	fanin	fanin	Yes
initial std	1.0	0.05	1.0	1.0	1.0	1.0
number of heads	-	-	4	-	-	4
dims per head	-	-	16	-	-	64
number of attention layers	-	-	4	-	-	2
max sequence length	-	-	5	-	-	1024